

CHAPTER 229

Environmental Assessment of Hypothetical Large-Scale Reclamation in Osaka Bay, Japan

Keiji Nakatsuji¹, Toshiaki Sueyoshi², Kohji Muraoka¹

ABSTRACT

In urban coastal areas in Japan, large-scale reclamation projects have recently increased, which have caused drastic changes in topographical features of the coastline. In Osaka Bay, the sea area of 5,200 ha have been reclaimed in the past 40 years and many development projects are under construction. As a natural consequence, the sea water has been polluted due to poor exchange of water with outer oceans and the load of nutritious substances discharged from rivers; hence, algal blooms occur independent of season and anoxia appears near the sea especially in summer. A 3-D baroclinic flow model is proposed to predict the tidally-interacting estuarine circulation and residual baroclinic currents in Osaka Bay and to evaluate the effects of hypothetical large-scale reclamation on the estuarine system.

INTRODUCTION

Osaka Bay is one of semi-enclosed urban coastal seas in Japan. High density populated and industrialized cities such as Osaka and Kobe are located at the head of Osaka Bay. The GNP (Gross National Product) of Osaka Prefecture approximately corresponds to that of Australia, in addition, the total amount of GNP of Osaka, Kobe and Kyoto does to that of Canada. Area of Osaka Bay is only 1400 km² and its mean depth is 28 m. In the past 40 years the coastal area of 5,200 ha have been reclaimed for satisfying the economical and industrial demand, and lots of development projects are under construction including a 511 ha for newly-built Kansai International Airport Island. As a result, the sea water has been polluted due to poor exchange of water with outer oceans and the load of nutritious substances from rivers; hence, algal blooms near the sea surface and anoxia near the sea bottom have

1 Dept. Civil Eng., Osaka University, Osaka 565, Japan.

2 Former student, Osaka University, Osaka 565, Japan

had adverse effects on fishery and recreation. Such a tendency, however, will have to continue because of the limited land and increasing volume of industrial and domestic waste products in the countries of their limited territory like Japan. Strategies for optimum environmental conservation must be examined in order to achieve integrated and multiple utilization of coastal seas in a sustainable manner.

Figure 1 shows a drastic change in topographical features of the coastline in Osaka Bay due to reclamation. The area of total reclaimed land is only 4 % against the total area of Osaka Bay at the present time. It, however, corresponds to 76 % as compared with the area of coastal waters shallower than 10 m depths. Such coastal area is of great importance for the special nursery of the fish and shellfish. Figure 2 shows the variation of shellfish catch with a cumulative area of reclaimed coastal area. It indicates that the reclamation causes strong damage to fishery.

Authors(1992) had already examined the impact assessment of large-scale reclamation on the tidal flow system and water quality transfer by the depth-integrated, two-dimensional finite element method. In the present study, since the density-induced current system is found to be of great importance, a three-dimensional baroclinic flow model is proposed to predict residual baroclinic currents and a tidal front observed in Osaka Bay and to evaluate the effects of hypothetical large-scale reclamation on the estuarine system.

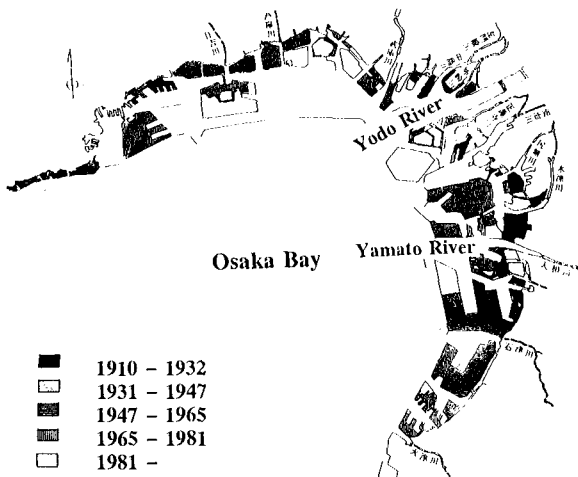


Figure 1. Change of shoreline due to reclamation projects in Osaka Bay.

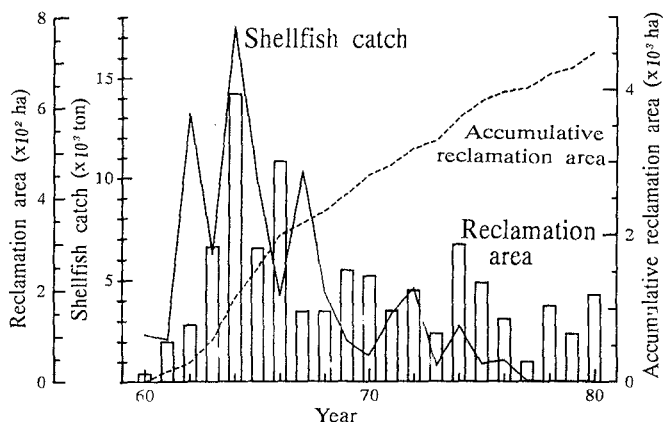


Figure 2. Variation of shellfish catch and cumulative area of reclamation.

MODEL DESCRIPTION

The computation solves the primitive equations of the ocean, governing the conservation of volume, momentum in three dimensions and density-difference simplified by the Boussinesq assumption and hydrostatic equilibrium.

$$\frac{\partial U}{\partial x} + \frac{\partial V}{\partial y} + \frac{\partial W}{\partial z} = 0 \quad (1)$$

$$\frac{DU}{Dt} - fV = -\frac{1}{\rho} \frac{\partial P}{\partial x} + \frac{\partial}{\partial x_i} (\epsilon_i \frac{\partial U}{\partial x_i}) \quad (2)$$

$$\frac{DV}{Dt} + fU = -\frac{1}{\rho} \frac{\partial P}{\partial y} + \frac{\partial}{\partial x_i} (\epsilon_i \frac{\partial V}{\partial x_i}) \quad (3)$$

$$0 = -g - \frac{1}{\rho} \frac{\partial P}{\partial z} \quad (4)$$

$$\frac{D\Delta\rho}{Dt} = \frac{\partial}{\partial x_i} (K_i \frac{\partial \Delta\rho}{\partial x_i}) \quad (5)$$

where (U, V, W) are velocities in the x, y and z directions, ζ is the water elevation, P is the pressure, $\Delta\rho (= \rho_s - \rho)$ is the density difference from the sea water density (ρ_s), D/Dt is a nonlinear operation such that $DA/Dt = \partial A/\partial t + \partial(UA)/\partial x + \partial(VA)/\partial y + \partial(WA)/\partial z$, ϵ_i and K_i are the

eddy viscosity and diffusivity coefficients respectively in each direction, and f is the Coriolis parameter ($0.8296 \times 10^{-4} \text{ s}^{-1}$). The pressure is obtained by integrating the vertical momentum equation (4) from the water surface ($z = -\zeta$) to any depth. Therefore, the pressure gradient $\partial P / \partial x_i$ can be expressed as a sum of the water surface gradient $\partial \zeta / \partial x_i$ (barotropic mode) and the density gradient $\partial \Delta \rho / \partial x_i$ (baroclinic mode).

A first-order closure scheme is used to account for the eddy viscosity and diffusivity coefficients. A small horizontal eddy viscosity or diffusivity ($20 \text{ m}^2/\text{s}$) is used in all model runs. On the other hand, the vertical eddy viscosity coefficient are affected by the reduction of turbulence due to stable stratification. On the basis of the study of three-dimensional buoyant surface discharges by Murota et al. (1989), the Webb formula (1970) and Munk and Anderson's formula (1948) are adopted for ϵ_z and K_z , with a neutral value of $\epsilon_{z_0} = 0.005 \text{ m}^2/\text{s}$. Both empirical formulae are functions of the gradient Richardson number, $Ri \equiv g(\partial \rho / \partial z) / (\partial U / \partial z)^2$ as follows;

$$\epsilon_z / \epsilon_{z_0} = (1 + 5.2 Ri)^{-1} \quad (6)$$

$$K_z / \epsilon_z = (1 + 10/3 \cdot Ri)^{-3/2} / (1 + 10 \cdot Ri)^{-1/2} \quad (7)$$

In the computation of tidal flow, however, turbulence energy in straits becomes unrealistically large. Hence, the values of $200 \text{ m}^2/\text{s}$ and $0.05 \text{ m}^2/\text{s}$ are used near the straits for horizontal and vertical eddy coefficients, respectively.

Boundary conditions are the following. The model basin is initially filled with saline sea water of 1022 kg/m^3 . Freshwater of zero salinity then flows near the surface from rivers located in the estuary head. The model ocean is everywhere bounded by solid vertical walls except the river mouth and the open seas.

Vertical walls are assumed impenetrative and slip, so that for solid boundary

$$\rho \epsilon_h \partial(U, V) / \partial x_h = \tau_h, \quad K_h \partial \Delta \rho / \partial x_h = 0, \quad V_n = 0 \quad \text{and} \quad \partial \Delta \rho / \partial x_n = 0 \quad (8)$$

where 'h' mean the normal and tangential components to the boundary and τ_h means the shear stress along the boundary.

At the river mouth, the time-variation of river discharges is given according to the observed hydrographs and the water elevation is assumed to be zero, so that

$$Q = Q(t), \quad \Delta \rho = 0.0, \quad \partial \zeta / \partial x_n = 0 \quad \text{at river mouth} \quad (9)$$

The open sea boundaries are

$$\partial(U, V) / \partial x_n = \partial \Delta \rho / \partial x_n = \zeta = 0 \quad (10)$$

When a tidal flow is taken into account, the time variation of tidal elevation is added on the basis of harmonic analysis of observed tidal elevation,

$$\partial(U, V) / \partial x_n = \partial \Delta \rho / \partial x_n = 0 \quad \text{and} \quad \zeta = \zeta(t) \quad (11)$$

On the free surface ($z = -\zeta$), fluxes of momentum and density are zero, so

$$\partial(U, V, \Delta \rho) / \partial z = 0 \quad \text{at} \quad z = -\zeta \quad (12)$$

On the ocean bottom ($z = H$), the momentum flux is balanced by a bottom stress τ_z , while the density flux and the vertical velocity are zero, so that

$$\rho \varepsilon_z \partial(U, V) / \partial z = \tau_z, \quad \partial \Delta \rho / \partial z = W = 0 \quad \text{at} \quad z = H \quad (13)$$

OUTLINE OF 3-D BAROCLINIC FLOW COMPUTATION

The algorithm and computational scheme was written in the authors' published paper. (See Murota, et al.(1988))

The computational domain as shown in Fig. 3 covers Osaka Bay and surrounding coastal seas, Sea of Harima and Ki-i Channel, in order to evaluate the amount of flowing through Akashi and Kitan Straits as precisely as possible. The model's resolution is 1 km in the horizontal plane with seven vertical layers having thickness of 2, 4, 6, 8, 10, 15 and 15 m. The time increment is 30 seconds.

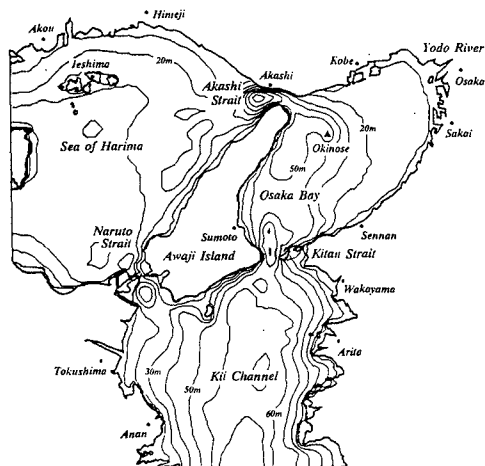


Figure 3. Topological features of Osaka Bay and computation domain

A semi-diurnal tide is represented by a sine-wave curve with a 12 hours cycle at two open boundaries. The amplitude and phase of tide are 36-39 cm and 330° at the boundary in Sea of Harima, and 46 cm and 174° at the boundary in Ki-i Channel according to the field surveys of the Ministry of Transportation. For the density-driven current, the average discharge and the density of the Yodo River was set to $205 \text{ m}^3/\text{s}$ and $0.997 \text{ kg}/\text{m}^3$ respectively. Another buoyancy flux is the thermal flux at the sea surface of $29.7 \text{ cal}/\text{s}/\text{m}^2$ in summer, which was also taken into account.

TIDAL FLOW PATTERN AND TIDAL FRONT IN OSAKA BAY

The computation results to be discussed here are that on the 36th tidal cycle, in which the change in the flow and density distributions over time is almost equivalent to those of the previous tidal cycle. Figure 4 shows the velocity and the density fields of the surface layer (1 m deep from the surface) when the eastward or westward flow through Akashi Strait reaches its maximum. The contours of density field are marked at every 10% of the density difference between the river water and sea water where $\sigma_t = 23$. When the eastward flow at Akashi Strait is at its maximum, the flow into Osaka Bay spreads in a jet-like form toward the southeast. The flow makes its way in clockwise circular arcs along a 20 m-deep contour line toward the Kitan Strait, off the coast of Sennan. Meanwhile the discharge from the Yodo River spreads southwest,

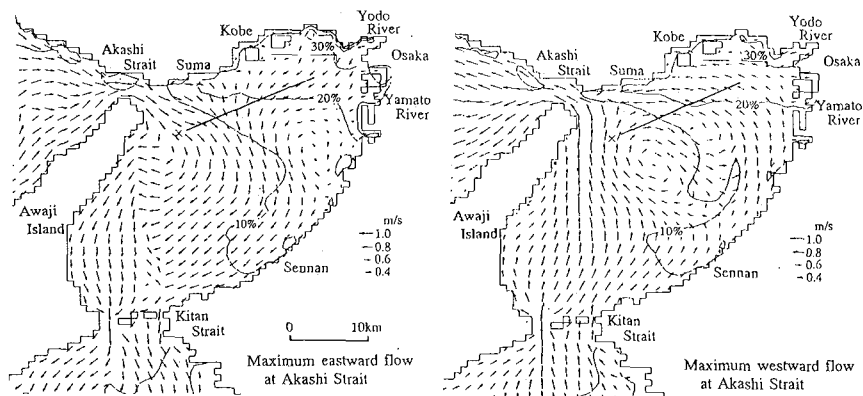


Figure 4. Surface flow vectors and density distribution at the maximum eastward and westward flow through the Akashi Strait.

running southward to cross the 20% density contour line at a right angle. The jet-like tidal flow from the Akashi Strait combines with this river discharge at the 20 m-deep point and continues southward.

When the westward flow is at its maximum, the water flow can roughly be divided into two: one running from the Kitan Strait northward along the east coast of Awaji Island, and the other that flows northward, off the coast of Sennan. Water from the Yodo River is carried by the tidal flow toward Kobe, a part of which flows into the Akashi Strait. The other part of the flow mixes with the circulation flow near Okino-se (indicated by X in Fig. 4). It is worth noting that the southeastward flow at Okino-se due to the eastward tidal flow persists even when the tidal flow direction changes. Between this southeastward flow and the flow in the inner bay, a discontinuous flow is observed. If the density distribution in Fig. 4 is represented in finer colour lines, the discontinuous boundary can be shown to be bands of different densities. That is a tidal front.

Figure 5 shows the density distribution at the cross-section of the tidal front, which is indicated by the solid line in Fig. 4. The horizontal 0 point corresponds to the 20 m-deep sea bed. The direction toward the inner bay (toward Osaka) is positive, and the direction toward the outer bay (toward Awaji Island) is negative. In the inner bay, approximately 5 m-thick stratification with $\sigma_t = 22$ or lower is observed. The stratification is stable, rarely affected by the change in the tidal flow. The area where the sea bed is deeper than 20 m ($x < 0$) is exposed to stronger tidal flows and, as a result, vertical mixing occurs. In this area σ_t is 22.5 or higher. Between these two areas, where σ_t is more than 20 and less than 22, density contours are almost perpendicular to the water surface.

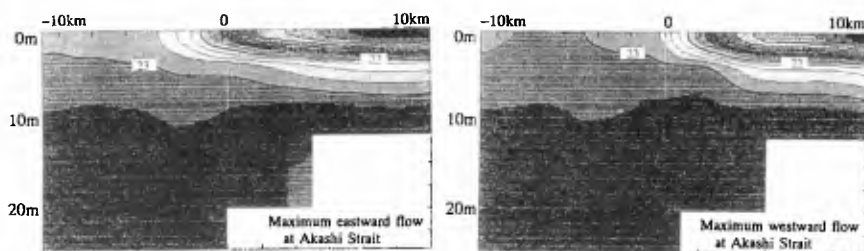


Figure 5. Density distribution at the section across tidal front at the maximum eastward and westward flow through the Akashi Strait.

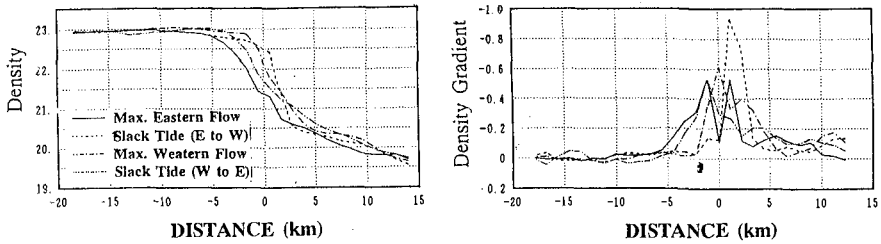


Figure 6. Surface density and its gradient distributions at the section across tidal front every three hours.

Figure 6 shows the horizontal distributions of surface density and its gradient every three hours. The gradient indicates the sharpness of the front. This figure shows that the tidal front on the cross section develops along the line connecting 20 m depth points. The density changes by $\sigma_t = 2$ over 7 km on this plane. The density gradient is the greatest when the eastward tidal flow through Akashi Strait reverses westward. At this time the front is 2 km wide and σ_t rises from the head to the center of the bay by $\sigma_t = 2$. It is because the eastward flow through Akashi Strait spreads deep into the head of bay. Field data obtained by Yanagi and Takahashi (1988) indicated the density change of $\sigma_t = 3$ over 5 km width of the tidal front. From these comparison, the computation results overestimate a little larger than observation ones.

RESIDUAL BAROCLINIC CURRENT SYSTEM

Figure 7 shows the residual current distribution in the first (-1 m) and third layers (-9 m). The residual current is calculated by integrating the flow velocity over one tidal cycle, that is, 12 hours. The residual current in the surface layer consists mainly of the Okino-se Circulation and the east-coast residual current offshore of Sennan. The figure especially at the surface shows higher velocities than the tidally-induced circulation. The remnants of the density-driven current generated by the inflow of the Yodo River spread only slightly from the river mouth to Suma. This density-driven current is caught by the edge of the Okino-se circulation, and as a result, it enhances the Okino-se circulation and the east coast residual current in their surface layers. In the third layer, where the influence of density-driven

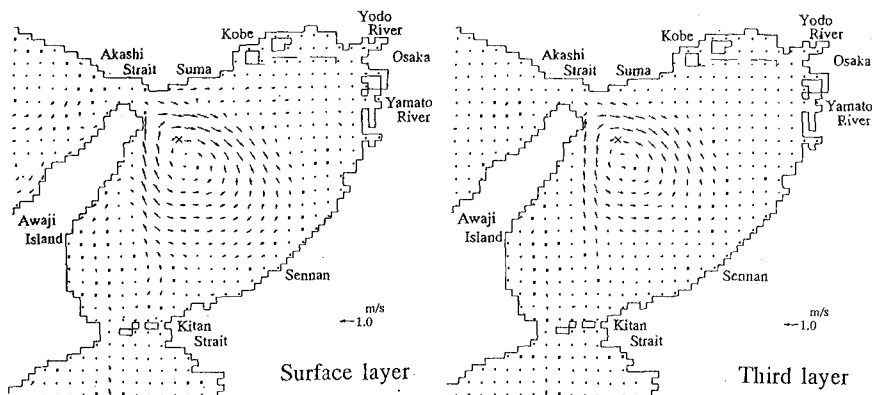


Figure 7. Residual baroclinic currents at the surface layer (-1 m) and the third layer (-9 m).

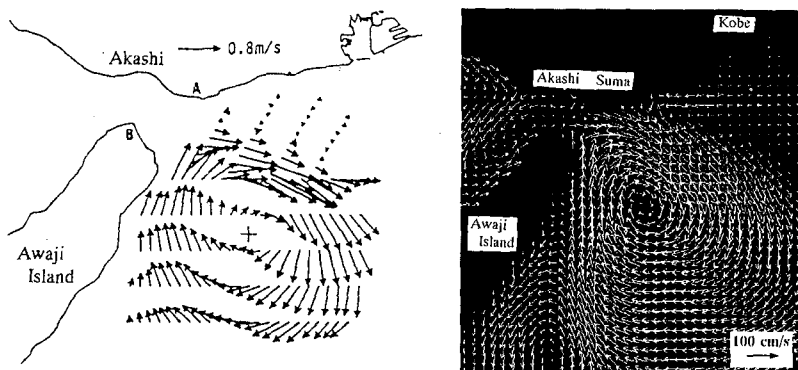


Figure 8. Observed residual current at 10 m depth corresponding to Okino-se Circulation and computed one at surface layer of 1 m depth.

current is less, there is a weak flow in the inner bay toward the Yodo River. Since the Okino-se circulation covers the surface to the bottom layers, they are assumed to be the remnants of the tidally-induced residual current. The strength of Okino-se circulation, therefore, changes depending on the tidal amplitude, but not on river discharges. According to the harmonic analysis of the time series of computed velocity fluctuation, it is found that the residual current component is possible to be larger than the tidal flow. (Nakatsuji et al.; 1994)

Figure 8 shows the comparison between residual current observed using four ADCP by Fujiwara et al.(1994) and computed one. Both results are substantial agreement with each other.

In order to understand the role of the residual current system on turbulent transport process, the numerical experiment was conducted that the four markers placed at the water surface near the Akashi Strait and inside Osaka Bay are traced by Lagrangian diffusion analysis based on Monte Carlo method. In this experiment, the spreading particles are assumed to move only at a surface layer.

If the particles are transformed by a tidal flow, they naturally return to their original points after one tidal cycle because the tidal flow behaves a periodic movement. As shown in Fig. 9, however, the computed tracers are far from their original positions and they remain in the center of Osaka Bay taking the shape of oval. After two tidal cycles, 24 hours, similar tendency can be observed. It suggests that the residual current system play a more important role on the transport process than the periodic tidal flow. Therefore, tracers are distributed with surrounding the Okino-se Circulation as a circle.

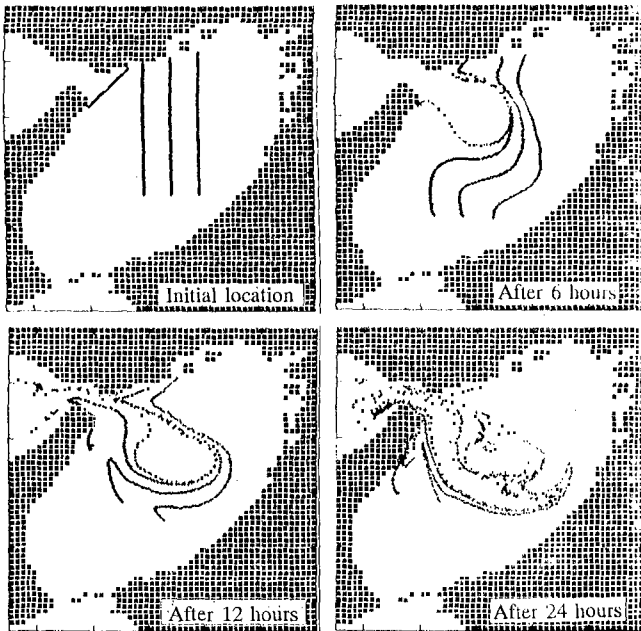


Figure 9. Computed trajectories of floating markers transported by the residual current system.

IMPACT ASSESSMENT OF HYPOTHETICAL LARGE-SCALE RECLAMATION

For examining the effects of hypothetical large scale reclamation on the flow movement and water quality transport, two simple reclamation topographies are assumed. They are the reclamation of coastal waters shallow than 15 m and 18 m. The decreasing rates in area and volume correspond to 26 % and 11 % for the reclamation shallow than 15 m depth, and 36 % and 20 % for that shallow than 18 m depth. It is of importance that the impact assessment must be established from the view point of long-term and circumstance of whole coastal seas. According to the above-mentioned discussion, the 'Okino-se Circulation' and the 'tidal front' can be adopted as the physical indexes for assessment.

Effects on Okino-se Circulation

Figure 10 shows the distribution of residual baroclinic current at the surface layer supposing the hypothetical reclamation could be constructed. The outer boundary in the west side is adjacent to the line connecting 20 m depth points, where the velocity of residual current becomes smaller in the rate of 10 % as compared with that in the case of present topography. And, no particular difference between the cases of 15 m or 18 m reclamation. Since the Okino-se Circulation occurs at all depths in all cases, it is a tidally-induced residual current; hence, it is a matter of course that the effects of reclamation inside the head of bay has not strongly affected on the Okino-se Circulation developed near the Akashi Strait.

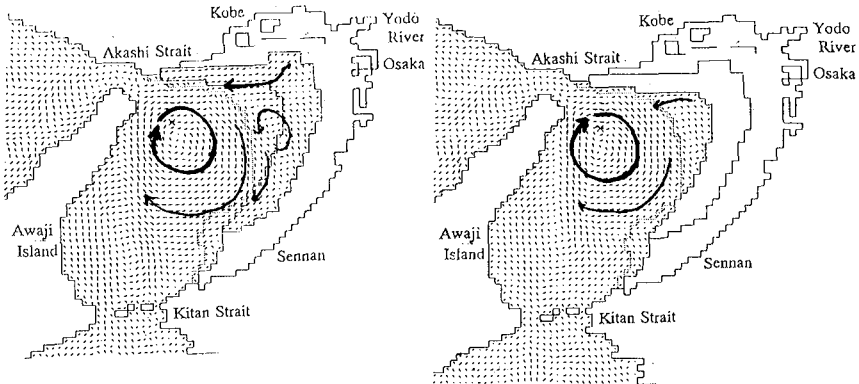


Figure 10. Residual baroclinic current at the surface layer in hypothetical reclamation of 15 m and 18 m depth.

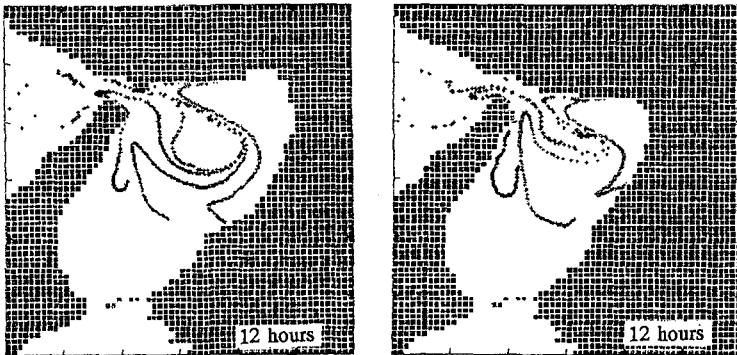


Figure 11. Computed trajectories of floating markers after one tidal cycle in reclamation of 15 m and 18 m depth.

Figure 11 shows the computed trajectories of four markers after one tidal cycle. As compared with Fig. 9, there is a little difference in the computed trajectories between the present topography and the reclamation of coastal seas shallower than 15 m. However, in the case of reclamation of 18 m depth, continuous ring-shaped markers are distorted to be pushed into the head of bay.

Effects on Tidal Front and Density Field

Accompanied with the reclamation in shallow coastal seas, the volume of river water has direct effects on the stratification in the eastern bay or mixing process. For example, the computation indicates that the thickness of stratified and upper layer in the head of Osaka Bay becomes 8 m. Its thickness is twice as large as that observed in the present topography.

Figures 12 and 13 show the comparison of density and its horizontal gradient at the sea surface across the tidal front along the solid line shown in Fig. 4. The axis of abscissas is the same as Fig. 5. The '0' point corresponds to the sea bed of 20 m depth. The positive value in the abscissas axis means the direction of eastern bay. The maximum value of density gradient and its horizontal point indicate the strength and location of the tidal front, respectively. The maximum value and its location are almost same between the present topography and the reclamation of 15 m depth. In addition, the density in the eastern sea ($x > 0$) is mixed to gradually change in the range of $\sigma_t = 19$ to 23 for the present topography and $\sigma_t = 18$ to 22 for the reclamation of 15 m depth.

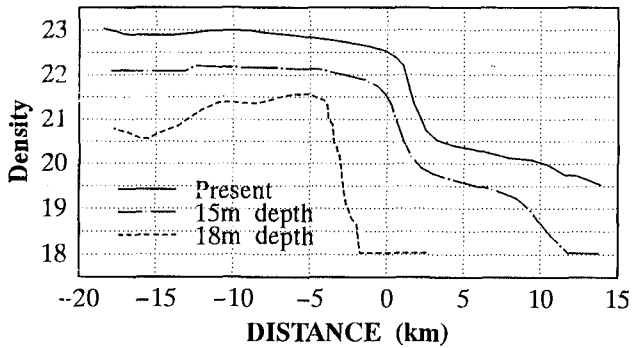


Figure 12. Distribution of surface density at the section across the tidal front against two reclamation cases.

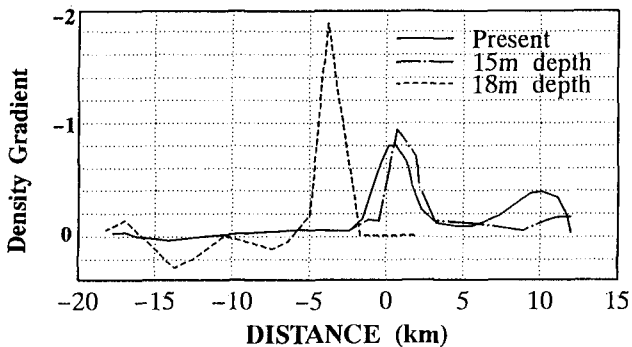


Figure 13. Change of location and intensity of tidal front depending on the gradient of density at the surface layer (-3 m).

On the other hand, in the case of reclamation of 18 m depth, the volume corresponding to about 20 % of whole Osaka Bay is lost; so that mixing between river water and sea water becomes decreased and remained in the head of bay. As a result, there is $\sigma_t = 18$ in the eastern sea, while $\sigma_t = 22.5$ in the western sea. A tidal front, therefore, develops in the narrow band of only 2.5 km. The maximum density gradient, namely the strength of tidal front, is twice as large as other cases. The location moves about 5 km in the western direction.

CONCLUSION

Through numerical experiments using a three-dimensional baroclinic flow model, the physical processes governing the flow movement and long-term mass transport processes in Osaka Bay, one of typical semi-enclosed coastal seas, are discussed. On the basis of discussion and the comparison of computation results with field observations, the 'Okino-se Circulation' and 'tidal front' are selected as the standards for examination of the impact assessment of hypothetical large scale reclamation in Osaka Bay. The computation results become clear from the physical viewpoint that the reclamation of coastal seas shallow than 15 m depth has not so strong effects on the flow movement and mass transfer processes, but that the reclamation of 18 m depth considerably affects them.

ACKNOWLEDGEMENT

Authors are indebted to Dr Tateki Fujiwara, Associate Professor of Department of Fishery, Kyoto University for providing useful discussion on residual current system in Osaka Bay.

REFERENCES

- Fujiwara, T., Sawada, Y., Nakatsuji, K. and Kuramoto, S. (1994). "Water exchange time and flow characteristics of the upper water in the easter Osaka Bay - Anticyclonic circulation in the head of the estuary." *Research Note on Coastal Seas, Oceanographical Society of Japan*, 31(2), 227-238. (in Japanese)
- Murota, A., Nakatsuji, K. and Huh, H.Y. (1988). "A numerical study of three-dimensional buoyant surface jet." *Proc. 6th APD-IAHR Congress*, 3, 57-64.
- Murota, A., Nakatsuji, K. and Huh, T.Y.. (1989). "A three-dimensional computer simulation model of river plume." *Refined Flow Modelling and Turbulence Measurements*, Ed. Y. Iwasa et al., University Academic Press, 539-547.
- Munk, W.H. and Anderson, E.R. (1970). "Notes on a theory of the thermocline," *J. Marine Res.*, 7, 276-295.
- Nakatsuji, K., J.Y. Huh and A. Murota (1991): "Numerical experiments of three-dimensional buoyant surface discharges," *Proc. JSCE*, 434/II-16, 29-36. (in Japanese)
- Nakatsuji, K., Karino, H., Kurita, H. and Muraoka, K. (1992). "Impact of Large-Scale Reclamaton on Tidal Current System and Water Quality Structure in Osaka Bay." *Hydraulic and Environmental Modelling : Coastal Waters*, Ed. R.A. Falconer et al., Ashgate, 43-53.

- Nakatsuji, K., Sueyoshi, T. and Fujiwara, T. (1994). "An estuarine system in semi-enclosed Osaka Bay." *Flux Change in Estuaries*, Ed. K. Dyer, Olsen and Olsen, 79-84.
- Webb, W.K. (1970). "Profile relationships, the log-linear range and extension to strong stability." *Quarterly J. Royal Meteorological Soc.*, 6, 67-90.
- Yanagi, T. and Takahashi, T. (1988). "A tidal front influenced by river discharges.", *Dynamics Atmosphere and Ocean*, 12, 191-206.